Stimulated radiative recombination and x-ray generation

A. Jaroń,[1] J. Z. Kamiński,[1] and F. Ehlotzky[2]
[1]Institute of Theoretical Physics, Warsaw University, Hoża 69, 00-681 Warszawa, Poland
[2]Institute for Theoretical Physics, University of Innsbruck, Technikerstrasse 25, A-6020 Innsbruck, Austria

(Received 3 August 1999; published 7 January 2000)

We consider the process of electron-ion recombination in a powerful laser field and investigate the spectrum of emitted x-ray radiation. This process is of interest in the interaction of laser radiation with gaseous or solid targets in connection with harmonic and coherent x-ray production. The process is treated in the framework of the inverse Keldysh-Faisal-Reiss model describing the ingoing electron either by a Gordon-Volkov wave or by a Coulomb-Volkov solution. Even for higher energies of the impinging electrons, considerable Coulomb effects are recognized. We evaluate the rates of the generated x-ray field and determine the energy range of its spectrum. The maximum photon energy achieved by this process is estimated by $\hbar\omega_X = E_{\mathbf{p}} + U_p + |E_B| + 2\sqrt{2U_pE_{\mathbf{p}}}$, with $E_{\mathbf{p}}$ being the kinetic energy of the ingoing electron, U_p the ponderomotive energy, and E_B the binding energy. The equivalence of the two models for the zero-range interaction is also shown.

PACS number(s): 32.80.Wr, 34.50.Rk, 42.50.Hz

I. INTRODUCTION

The radiative recombination of a positive ion and an electron with subsequent emission of a photon, $A^{+n}+e^- \rightarrow A^{+(n-1)}+\hbar\omega$, has been a subject of thorough studies in plasma physics and astrophysics for the past 70 years [1]. From a theoretical point of view, the process is the inverse of photoionization. Direct experimental observation of the isolated recombination process was extremely difficult due to its small cross section. The situation has changed when the use of merged electron and ion beams in storage rings enabled the performance of very precise measurements. Ions stored in a ring and electrons of a cooling beam, propagating with equal average velocities and proper spatial overlap, may undergo collisions which give rise to spontaneous recombination accompanied by photon emission. The rate of recombination can be significantly enhanced by the presence of an external field and this process is called stimulated radiative recombination or laser-induced radiative recombination. For example, a process of this type, the formation of hydrogen, was observed during electron cooling of a proton beam in a storage ring and the total rate of the recombination was measured as well as the so-called gain factor, representing the induced recombination rate normalized to the spontaneous rate, as a function of the laser intensity and wavelength [2,3]. In particular, a gain factor of the order of 1000 has been measured for hydrogen formation with final states of the principal quantum numbers $n=11$, 12, and 13 [4]. Further studies of the photorecombination spectrum have been stimulated by promising prospects of the future application of the laser-induced recombination for producing recombined systems in desired, well-defined final states [5]. Finally, laser-induced recombination was studied with the hope of future exploitation in designing short-wavelength lasers pumped by recombination. The intensive search for new lasers and the challenge to extend the region of known laser lines into the x-ray domain has led to the investigation of high-density plasmas as possible active media [6]. In particular, it has been realized that in addition to high harmonic generation from gaseous targets, x-ray radiation can be efficiently generated from high-power laser interactions with solid surfaces [7]. In this case both odd and even harmonics are generated via the oscillating electric current associated with electrons being dragged back and forth across the asymmetric density distribution created at the surface. Moreover, for low-energy electrons the problem of stimulated recombination at a resonance was investigated in [8], where the number of pairs recombined by a laser pulse was analyzed as a function of the laser field parameters.

Very promising conditions for x-ray generation by means of laser field-induced electron-ion recombination can be met in the experimental setup, proposed many years ago by Farkas and Horváth [9], as depicted in Fig. 1. In such a setup, very short and powerful x-ray pulses may be generated by shining laser light at grazing incidence on a gold target to create a surface plasma and by applying in addition a strong static negative voltage to a metal plate parallel to the gold target at a small distance of about 1 cm such that electrons are pushed back to the gold surface. If picosecond laser pulses of some 10^{12} W/cm^2 are focused onto the target and a static voltage of some 20 kV is applied, x-ray radiation of about 20 keV is observed at a power of some 20 mRtg per pulse. The appearance of these x-ray pulses coincides exactly with the laser pulses and these x-ray pulses emanate only from the laser spot at the metal surface. No x-ray emission

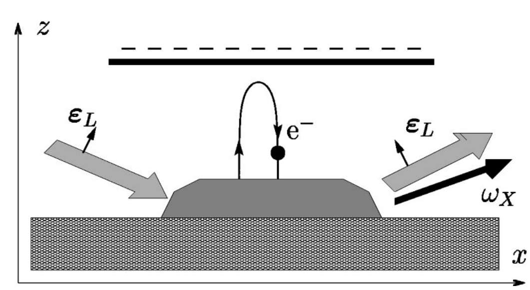

FIG. 1. Sketch of the Farkas and Horváth experimental setup. The laser pulse shining at grazing incidence on a gold target creates a surface plasma. Energetic electrons, which normally escape from the plasma, are pushed back by a constant negative voltage and recombine with ions generating at the same time x-ray radiation.

from other surfaces of the experimental setup is detected. At the same time an extremely high electron current density towards the cathode is measured. These strong Röntgen pulses are, however, not observed in the absence of the strong static electric field. Hence this scheme presents a rather simple means to produce strong x-ray fields with rather modest costs of the equipment. The above experiments have been repeated with essentially the same conclusions by Dinev *et al.* [10] and by Hontzopoulos *et al.* [11]. The observed x-ray pulses have a rather complicated structure and a certain part of it can be explained by electron bremsstrahlung emission and electron-ion recombination.

To summarize, in order to utilize high-energy electrons which are produced not only by means of multiphoton ionization of atoms [12] but also by some collective electron-plasma interaction effects [13,14], a static high voltage is applied [9] that pushes back fast electrons towards the target and allows them to recombine with plasma ions and hence to radiate x-ray photons. In particular, in this manner one can make use of hot electrons produced in above-threshold ionization, since it is now a well-established experimental [15] and theoretical [16] fact that in multiphoton ionization in a powerful laser beam the electron spectrum extends up to $10U_p$ (U_p being the ponderomotive energy), and that the physical mechanism responsible for this is the rescattering of slow photoelectrons by their parent ions in the presence of the laser field. Hot electrons of the energy around $10U_p$ are predominantly moving in the direction of polarization of the linearly polarized laser beam. Usually, these electrons are lost for the x-ray generation. The experimental setup of Farkas and Horváth prevents such an escape and creates the possibility to further extend the energy spectrum of high harmonics. The aim of this paper is to study such a possibility.

II. COULOMB-VOLKOV MODEL FOR RECOMBINATION

Let us consider the process of recombination of electrons with ions in the presence of a strong laser beam, described by a vector potential $\boldsymbol{A}_L(t)$ in the dipole approximation. During the action of the laser field, the emission of x-ray photons of frequency ω_X, wave vector $(\omega_X/c)\boldsymbol{n}$, and linear polarization $\boldsymbol{\varepsilon}$ takes place. In the electric field gauge the differential power spectrum of high-energy photons radiated into the solid angle $d\Omega_{\boldsymbol{n}}$ is given in atomic units by the following formula:

$$S(\omega_X,\boldsymbol{n},\boldsymbol{p})=\frac{\alpha\omega_X^4 p}{(2\pi)^4c^2}\left|\frac{\omega_L}{2\pi}\int_0^{2\pi/\omega_L}dt I(t)\right|^2, \qquad (1)$$

where α, $\boldsymbol{c}$, and $\boldsymbol{p}$ are the fine-structure constant, speed of light, and the momentum of incident electrons, respectively, whereas

$$I(t)=\int d\boldsymbol{r}\psi_B^*(\boldsymbol{r},t)\boldsymbol{\varepsilon}\cdot\boldsymbol{r}e^{i[\omega_X t-(\omega_X/c)\boldsymbol{n}\cdot\boldsymbol{r}]}\psi_{\boldsymbol{p}}^{(+)}(\boldsymbol{r},t). \qquad (2)$$

Here, $\psi_B(\boldsymbol{r},t)$ is the wave function of a final quasibound state of an electron in the laser field and $\psi_{\boldsymbol{p}}^{(+)}(\boldsymbol{r},t)$ is the scattering state of an electron in both the laser field and the static binding potential of an ion. We shall further assume that $\psi_B(\boldsymbol{r},t)$ is a wave function of the ground state of an electron without the laser field, which for hydrogen takes the form

$$\psi_B(\boldsymbol{r},t)\approx\sqrt{\frac{\beta^3}{\pi}}e^{-iE_Bt}e^{-\beta r}, \qquad (3)$$

with $\beta=1$ and $E_B=-0.5$ in atomic units, and that $\psi_{\boldsymbol{p}}^{(+)}(\boldsymbol{r},t)$ is represented by the Coulomb-Volkov solution

$$\psi_{\boldsymbol{p}}^{(+)}(\boldsymbol{r},t)\approx\exp\left(-iE_{\boldsymbol{p}}t-i\boldsymbol{\alpha}_L(t)\cdot\boldsymbol{p}-\frac{i}{2m}\int^t e^2\boldsymbol{A}_L^2(t)dt\right)u_{\boldsymbol{p}-e\boldsymbol{A}_L(t)}^{(+)}(\boldsymbol{r}), \qquad (4)$$

where $u_{\boldsymbol{p}}^{(+)}(\boldsymbol{r})$ is the Coulomb scattering state without the laser field. The laser field is assumed to be described by the following vector potential: $\boldsymbol{A}_L(t)=\boldsymbol{A}_0\cos\omega_L t$. Hence, in the above equation, $\boldsymbol{\alpha}_L(t)=\boldsymbol{\alpha}_0\sin\omega_L t$ with $\boldsymbol{\alpha}_0=-e\boldsymbol{A}_0/\omega_L$. The first approximation, Eq. (3), is commonly applied in the KFR models [17], whereas the second one, Eq. (4), is justified for high-energy electrons considered here [18,19].

Figure 2 presents the differential power spectrum $\boldsymbol{S}$ as a function of the emitted x-ray photon energy $\hbar\omega_X$ for the electron energy $E_{\boldsymbol{p}}=42.5$ a.u. and for three intensities of an Nd:YAG (yttrium aluminum garnet) laser field of $\hbar\omega_L=1.17$eV. We observe the emergence of a plateau, bounded both from below and above, the width of which increases with intensity of the laser beam. Moreover, its maximum value slightly decreases with intensity, which does not take place for the well-known high harmonic plateau [20] .

III. KFR MODEL FOR RECOMBINATION

In order to understand qualitatively the above results, we have compared our model with the Keldysh-Faisal-Reiss model in which the scattering state in the laser field is approximated by the corresponding Gordon-Volkov solution. We present in Figs. 3 and 4 the differential power spectra calculated with the Coulomb-Volkov wave function, Eq. (4), and the Gordon-Volkov plane wave, respectively. We observe, as expected, that with increasing electron energy the results of both models converge. However, even for $E_{\boldsymbol{p}}$ around 1000 eV, the difference is still visible. Quite surprisingly, the inclusion of the effect of the attracting Coulomb potential diminishes the emitted power spectrum, which is in contrast to the multiphoton ionization rates, where we observe a substantial enhancement by the presence of the Coulomb attraction [19]. This could be an explanation for the fact that the commonly used strong field approximation for high harmonic generation [21] provides a reasonable agreement with both experimental and numerical data, although the two basic ingredients of this model (that is, ionization and capture) are not satisfactorily described by the plane-wave approximation for the laser dressed electrons in the continuum with rather small kinetic energies (see, e.g., [22]).

We consequently see that although there is a difference between these two models, nonetheless the structure of the

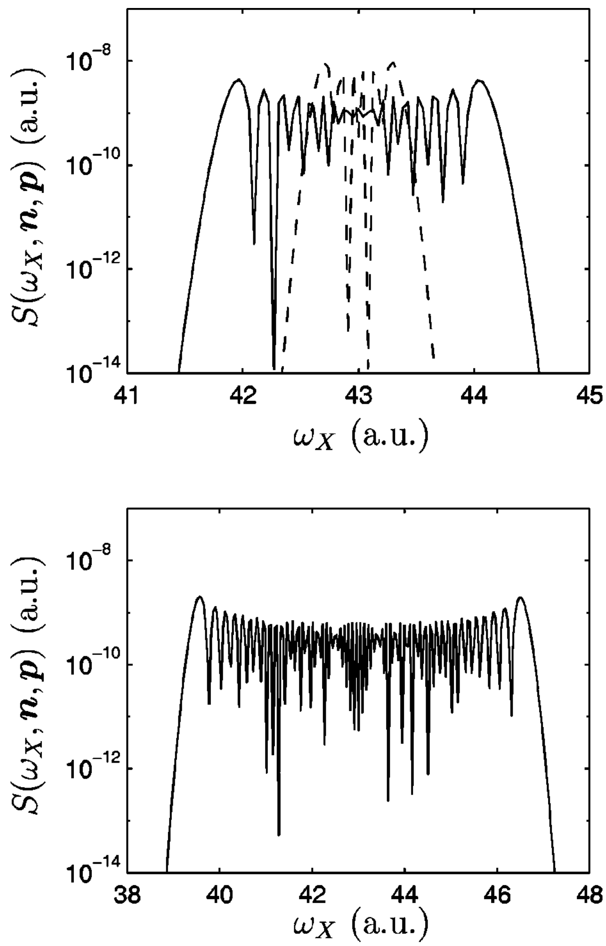

FIG. 2. Differential power spectrum calculated with the Coulomb-Volkov state for the geometry, in which the laser beam and the generated x-ray radiation propagate along the x direction, the polarization vectors are parallel to the $\boldsymbol{z}$ direction, whereas the electron momentum vector is antiparallel to the $\boldsymbol{z}$ direction (see Fig. 1). The laser photon energy is equal to $\hbar\omega_L = 1.17$ eV and the electron kinetic energy is $E_{\boldsymbol{p}} = 42.5$ in atomic units. In the upper frame, the differential power spectrum is presented for lower laser field intensities, i.e., for $I = 10^{11}$ W/cm^2 (dash line) and for $I = 10^{12}$ W/cm^2 (full line), and in the lower frame for the higher intensity $I = 10^{13}$ W/cm^2. Observe the formation of a plateau, bounded both from below and above, the width of which increases, whereas the magnitude of the differential power spectrum slightly decreases at the same time with increasing laser field intensity. For a given $E_{\boldsymbol{p}}$ the power spectrum exists only for some discrete values of $\hbar\omega_X$, which fulfill the energy conservation condition, Eq. (6). For visualization purposes, the points are connected by lines.

plateau qualitatively remains the same. Therefore, in order to understand how the x rays' plateau depends on the laser field parameters and on the electron energies, we have replaced in our formulas the Coulomb-Volkov state by the Gordon-Volkov wave function and have moreover assumed that both the electron kinetic energy $E_{\boldsymbol{p}}$ and momentum $\boldsymbol{p}$ are much larger than the ponderomotive energy U_p and x-ray photon momentum $(\omega_X/c)\boldsymbol{n}$, respectively. With these approximations we finally arrive at the following approximate formula for the differential power spectrum:

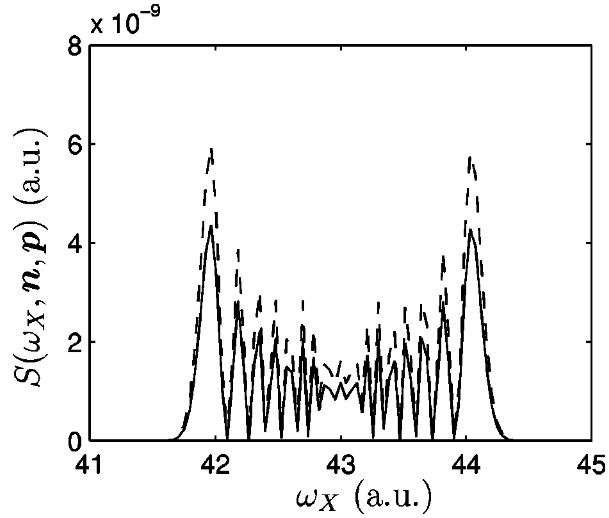

FIG. 3. Comparison of the differential power spectra calculated for the Coulomb-Volkov state (full line) and the Gordon-Volkov plane wave (dash line), respectively, for the same geometry, laser photon energy, and electron energy as in Fig. 2, and for the laser field intensity $I = 10^{13}$ W/cm^2. Observe that even for such a large electron energy, the difference between these two approaches is still visible.

$$S(\omega_X, \boldsymbol{n}, \boldsymbol{p}) = \frac{2^6 \alpha \beta^5 \omega_X^4 p}{\pi^3 c^2} \frac{(\boldsymbol{\varepsilon}\cdot\boldsymbol{p})^2}{(\beta^2 + \boldsymbol{p}^2)^6} J_n^2(\boldsymbol{\alpha}_0 \cdot \boldsymbol{p}), \tag{5}$$

in which $\boldsymbol{n}$ is determined by the energy conservation condition

$$\omega_X = E_{\boldsymbol{p}} + U_p + |E_B| + n\omega_L. \tag{6}$$

It has to be noted, however, that the above simple formula for the differential power spectrum can only be used for a qualitative analysis of the x-ray power spectrum for electron energies even up to 1000 eV, for which the difference be-

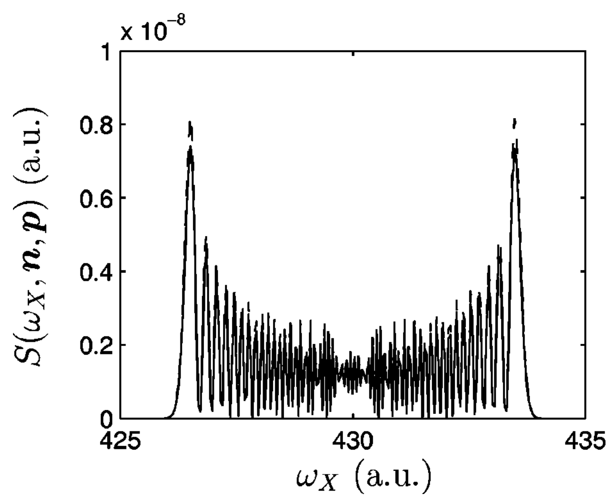

FIG. 4. The same as in Fig. 3, but for the larger electron energy $E_{\boldsymbol{p}} = 429.5$ in atomic units. As expected, discrepancies between these two models decrease with increasing electron energy.

tween the data of the two models, considered here, approaches approximately 20% at the edges of the spectrum.

Considering, in particular, the geometry in which $\boldsymbol{\alpha}_0 || \boldsymbol{p}$, we want to find an estimate of the domain for which the power spectrum attains significant values. The corresponding limits are given by the condition $|n| \leqslant \alpha_0 p$, i.e., when

$$|n|\omega_L \leqslant \alpha_0 \omega_L \sqrt{2mE_{\boldsymbol{p}}} = 2\sqrt{2U_p E_{\boldsymbol{p}}}. \tag{7}$$

This condition, which follows from the well-known properties of the Bessel functions of large indices and arguments, determines the possible frequencies of the emitted x-ray photon (i.e., frequencies for which the power spectrum attains significant values), provided we account for the energy conservation condition, Eq. (6),

$$E_{\boldsymbol{p}} + U_p + |E_B| - 2\sqrt{2U_p E_{\boldsymbol{p}}} \leqslant \omega_X \leqslant E_{\boldsymbol{p}} + U_p + |E_B| + 2\sqrt{2U_p E_{\boldsymbol{p}}}. \tag{8}$$

From the above considerations, we can conclude that the shape of the power spectrum forms a plateau, centered around $\omega_X = E_{\boldsymbol{p}} + U_p + |E_B|$, the width of which is equal to $\Delta\omega_X = 4\sqrt{2U_p E_{\boldsymbol{p}}}$ and grows with increasing laser field intensity. The power spectrum attains its maxima at the edges of this plateau. In Fig. 5 we present the contour plot of the differential power spectrum $\boldsymbol{S}$, calculated for the Coulomb-Volkov state, in the $(E_{\boldsymbol{p}}, \omega_X)$ plane. One can clearly see the region of dominant x-ray radiation production. The positions and shapes of the two edges are well described by the above formulas, although the energy $E_{\boldsymbol{p}}$ considered here is not much larger than the ponderomotive energy, U_p, as well as the ionization energy, $|E_B|$. For the KFR model, a qualitatively similar contour plot appears, with the same positions of the edges of the spectrum.

Our approximate formula, Eq. (5), shows that the most favorable conditions for the generation of x rays are with all vectors $\boldsymbol{\varepsilon}$, $\boldsymbol{\alpha}_0$, and $\boldsymbol{p}$ parallel to each other. This simple model also explains why with increasing laser field intensity the differential power spectrum slightly decreases. It follows from the asymptotic behavior of the Bessel functions $J_n(n)$ for large $\boldsymbol{n}$ [23],

$$J_n(n) \sim \frac{2^{1/3}}{3^{2/3}\Gamma(2/3)} n^{-1/3}, \tag{9}$$

where $\Gamma(z)$ is Euler's gamma function. Since in our case $n\omega_L \approx 2\sqrt{2U_p E_{\boldsymbol{p}}}$, we find for a given electron kinetic energy $E_{\boldsymbol{p}}$ (but much larger than the ponderomotive energy U_p) and particular laser photon energy ω_L that the differential power spectrum drops down with increasing laser field intensity $\boldsymbol{I}$ like

$$S(\omega_X, \boldsymbol{n}, \boldsymbol{p}) \sim I^{-1/3}. \tag{10}$$

This fact does not mean, however, that for large laser field intensities the suppression of the power of emitted x rays could be observed. The power spectrum presented here is calculated for a single recombination event. Since the number of such events grows rapidly with increasing laser field intensity, due to the increase of the number of electrons and ions created in the process of plasma formation in a laser field, we can, therefore, expect that the power of high-energy photons will also rapidly increase with the laser intensity. At present, it is difficult to determine this power since the number and the momentum distribution of hot electrons in a plasma are not precisely known. However, in order to roughly estimate the energy conversion efficiency, let us make the following qualitative analysis. It is an experimental fact that the energy conversion efficiency for high-order harmonics generated in the first dominant plateau, which ends at photon energies close to $3U_p$, is of the order of 10^{-6} [7]. On the other hand, experiments measuring hot electrons, as well as theoretical analysis, show that the ratio of the number of electrons with energy equal to $10U_p$ to the number of slow electrons is of the order of 10^{-5} [15,16]. Using these numbers, and noticing that for a broad range of electron energies

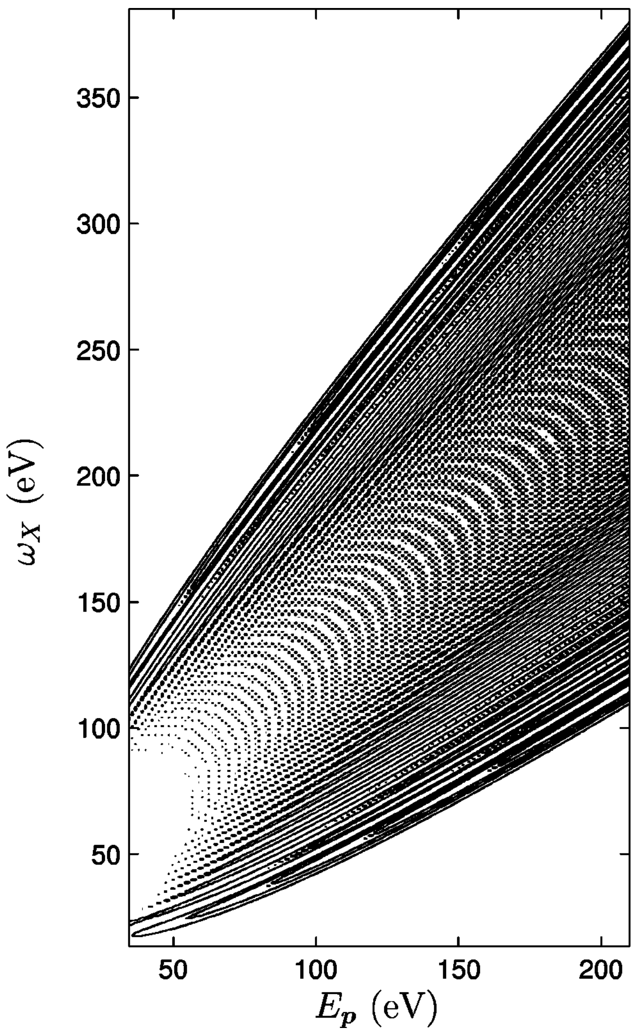

FIG. 5. Contour plot of the differential power spectrum in the $(E_{\boldsymbol{p}}, \omega_X)$ plane calculated with the Coulomb-Volkov state for the same geometry and laser photon energy as in Fig. 2, but for the laser intensity $I = 10^{14}$ W/cm^2. The limiting lines are well reproduced by the formulas $\omega_X = E_{\boldsymbol{p}} + U_p + |E_B| - 2\sqrt{2U_p E_{\boldsymbol{p}}}$ (for the lower edge) and $\omega_X = E_{\boldsymbol{p}} + U_p + |E_B| + 2\sqrt{2U_p E_{\boldsymbol{p}}}$ (for the upper edge).

the recombination probability rates are of the same order of magnitude, we estimate that the energy conversion efficiency of x-ray radiation of energy around $20U_p$ (i.e., for $E_{\boldsymbol{p}} \approx 10U_p$) could be of the order of 10^{-11}.

IV. EQUIVALENCE OF THE TWO MODELS FOR ZERO-RANGE INTERACTION

The Coulomb potential is one of very few examples of interactions for which the exact scattering wave function $u_{\boldsymbol{p}}^{(+)}(\boldsymbol{r})$ can be written in a closed form. Due to this fact, the space integration that appears in the expression for the differential power spectrum, Eq. (2), can be performed exactly. Another example of such an interaction is the zero-range interaction. In the three-dimensional space it can be defined by a potential of the form [24–26]

$$V(r)=\sqrt{\frac{2\pi^2}{|E_B|}}\delta(\boldsymbol{r})\frac{\partial}{\partial r}r, \tag{11}$$

where $\delta(\boldsymbol{r})$ is the three-dimensional Dirac δ distribution. For the above interaction, a particle possesses one bound state of energy $E_B=-|E_B|$, and the wave function of this state takes the form

$$\psi_B(\boldsymbol{r})=\sqrt[4]{\frac{|E_B|}{2\pi^2}}\frac{\exp(-\sqrt{2|E_B|}r)}{r}. \tag{12}$$

Also the scattering state can be written down in closed form,

$$u_{\boldsymbol{p}}^{(+)}(\boldsymbol{r})=e^{i\boldsymbol{p}\cdot\boldsymbol{r}}+f(p)\frac{e^{ipr}}{r}, \tag{13}$$

where the scattering amplitude $f(p)$ is equal to

$$f(p)=\frac{i}{p-i\sqrt{2|E_B|}}. \tag{14}$$

This potential is broadly applied in studies of the interaction of low-energy electrons with neutral atoms provided that the de Broglie wavelength of a free electron is much larger (i.e., the kinetic energy is sufficiently small) than the size of an atom. One can ask, therefore, what is the difference between the two models for x-ray generation considered in this paper, when electrons interact with neutral atoms? If we apply the dipole approximation to the x-ray radiation, which is very much justified for the x-ray frequencies considered above, the function $I(t)$, defined by Eq. (2), adopts the form

$$\begin{aligned}I(t)=&\sqrt[4]{\frac{|E_B|}{2\pi^2}}\exp\bigg(i[E_B-E_{\boldsymbol{p}}-\boldsymbol{\alpha}_L(t)\cdot\boldsymbol{p}]\\&-\frac{i}{2m}\int^t e^2\boldsymbol{A}_L^2(t)dt\bigg)\int d\boldsymbol{r}\frac{\exp(-\sqrt{2|E_B|}r)}{r}\boldsymbol{\varepsilon}\cdot\boldsymbol{r}\\&\times\bigg(e^{i[\boldsymbol{p}-e\boldsymbol{A}_L(t)]\cdot\boldsymbol{r}}+f[|\boldsymbol{p}-e\boldsymbol{A}_L(t)|]\\&\times\frac{\exp[i|\boldsymbol{p}-e\boldsymbol{A}_L(t)|r]}{r}\bigg).\end{aligned} \tag{15}$$

It is clearly seen that after space integration the only nonvanishing contribution comes from the plane-wave part of the scattering state, as it is assumed in the KFR models. This means that for the zero-range interaction, or more generally for an interaction the range of which is much smaller than the de Broglie wavelength of recombined electrons, both approaches presented here are equivalent. Obviously, the same analysis can be applied to the ionization process as well as to the high harmonic generation, because also in these cases the space integrations yield only the plane-wave part of the exact scattering state (cf., [19,22]). This means, in particular, that for very short-range interactions (more precisely, the range should be much less than the de Broglie wavelength of free electrons), both models, i.e., ours, with the modified exact scattering state, and the KFR model, give exactly the same results. The situation changes if one deals with long-range interactions. As follows from our previous investigations [19,22] and the analysis presented in this paper, accounting for the Coulomb interaction modifies multiphoton processes in strong laser fields, if compared to the KFR models, even for electron energies as large as 1000 eV.

V. CONCLUSIONS

In view of existing considerations, mentioned in the Introduction, that electron-ion recombination in a laser field could be another potential source for generating x rays of increasingly higher coherent photon energy, we investigated in the present work this stimulated recombination process in the framework of the inverse KFR model, taking into account the Coulomb effects of the ionic target on the ingoing laser-dressed electron. These Coulomb effects were found to be considerable even at higher electron kinetic energies. We evaluated on the basis of our model the rates and estimated their orders of magnitude for the generated discrete x-ray spectrum. We also determined the dominant frequency range of this x-ray field and evaluated the laser intensity dependence of the rates of electron-ion recombination. In conclusion, we estimated that the energy conversion efficiency of x-ray radiation of about $20U_p$ will be of the order of magnitude 10^{-11}. Finally, we showed that our model, with the laser dressed exact scattering state of an electron interacting with an atom, is equivalent to the KFR model provided that the static electron-atom interaction can be approximated by a zero-range potential. This equivalence holds for photoionization, stimulated recombination, as well as for high harmonic generation processes.

ACKNOWLEDGMENTS

This work was supported by the Scientific-Technical Collaboration Agreement between Austria and Poland for 1998/99 under Project No. 18/98 and by the East-West-Program of the Austrian Academy of Sciences and the Austrian Ministry of Science and Transportation under Project No. 45.372/2-IV/6/97. A.J. and J.Z.K. acknowledge support by the Polish Committee for Scientific Research (Grant No. KBN 2 P03B 007 13) and use of the computer facilities at the Computation Center (ICM) of Warsaw University. A.J. was supported by Stypendium dla Młodych Naukowców Fundacji na rzecz Nauki Polskiej.

[1] Y. Hahn, Rep. Prog. Phys. **60**, 691 (1997).

[2] H. Poth *et al.*, Z. Phys. A **332**, 171 (1989); Phys. Rep. **196**, 135 (1990).

[3] U. Schramm *et al.*, Phys. Rev. Lett. **67**, 22 (1991).

[4] M. L. Rogelstad, F. B. Yousif, T. J. Morgan, and J. B. A. Mitchel, J. Phys. B **30**, 3913 (1997).

[5] T. Schüssler, *et al.*, Phys. Rev. Lett. **75**, 802 (1995).

[6] A. V. Borowskii, E. V. Chizhonkov, A. L. Galkin, and V. V. Korobkin, Appl. Phys. B: Photophys. Laser Chem. **50**, 297 (1990); J. Zhang, M. H. Key, S. J. Rose, and G. J. Tallents, Phys. Rev. A **49**, 4024 (1994); M. J. Grout, G. J. Pert, and A. Duaoui, J. Phys. B **31**, 197 (1998).

[7] P. A. Norreys *et al.*, Phys. Rev. Lett. **76**, 1832 (1996), and references therein.

[8] F. H. M. Faisal, A. Lami, and N. K. Rahman, J. Phys. B **14**, L569 (1981); A. Lami, N. K. Rahman, and F. H. M. Faisal, Phys. Rev. A **30**, 2433 (1984); P. Schlagheck, P. Maragakic, and P. Lambropoulos, Z. Phys. D: At., Mol. Clusters **37**, 19 (1996).

[9] Gy. Farkas and Z. Gy. Horváth, Opt. Commun. **21**, 408 (1977).

[10] S. G. Dinev, Ch. I. Radev, K. V. Stamenov, and K. A. Stankov, Opt. Commun. **30**, 219 (1979); Opt. Quantum Electron. **12**, 231 (1980).

[11] E. Hontzopoulos, D. Charalambidis, C. Fotakis, Gy. Farkas, Z. Gy. Horváth, and Cs. Tóth, Opt. Commun. **67**, 124 (1988).

[12] The possibility of generating x rays and fast electrons produced upon interaction of powerful picosecond and subpicosecond laser pulses with solid targets in vacuum was reviewed by M. D. Perry and G. Mourou, Science **264**, 917 (1994).

[13] S. Varró and F. Ehlotzky, Phys. Rev. A **57**, 663 (1998).

[14] S. Varró and F. Ehlotzky, J. Phys. D **30**, 3071 (1997).

[15] K. J. Schafer, B. Yang, L. F. DiMauro, and K. C. Kulander, Phys. Rev. Lett. **70**, 1599 (1993); B. Yang, K. J. Schafer, B. Walker, K. C. Kulander, P. Agostini, and L. F. DiMauro, *ibid.* **71**, 3770 (1993); G. G. Paulus, W. Nicklich, H. Xu, P. Lambropoulos, and H. Walther, *ibid.* **72**, 2851 (1994); G. G. Paulus, W. Nicklich, and H. Walther, Europhys. Lett. **27**, 267 (1994); M. J. Nandor, M. A. Walker, and L. D. Van Woerkom, J. Phys. B **31**, 4617 (1998).

[16] A. Lohr, M. Kleber, R. Kobold, and W. Becker, Phys. Rev. A **55**, R4003 (1997); D. B. Milošević and F. Ehlotzky, *ibid.* **58**, 3124 (1998); F. H. M. Faisal and A. Becker, Laser Phys. **7**, 684 (1997).

[17] L. V. Keldysh, Zh. Éksp. Teor. Fiz. **47**, 1945 (1964) [Sov. Phys. JETP **20**, 1307 (1965)]; F. H. M. Faisal, J. Phys. B **6**, L89 (1973); H. R. Reiss, Phys. Rev. A **22**, 1786 (1980).

[18] N. M. Kroll and K. M. Watson, Phys. Rev. A **8**, 804 (1973).

[19] J. Z. Kamiński, A. Jaroń, and F. Ehlotzky, Phys. Rev. A **53**, 1756 (1996); A. Jaroń, J. Z. Kamiński, and F. Ehlotzky, Opt. Commun. **163**, 115 (1999).

[20] See, e.g., C. G. Wahlström, Phys. Scr. **49**, 201 (1994), and references therein.

[21] F. Ehlotzky, Nuovo Cimento D **14**, 517 (1992); W. Becker, S. Long, and J. K. McIver, Phys. Rev. A **50**, 1540 (1995); P. Saliéres, A. L'Huillier, and M. Lewenstein, Phys. Rev. Lett. **75**, 3376 (1995), and references therein.

[22] J. Z. Kamiński and F. Ehlotzky, Phys. Rev. A **54**, 3678 (1996).

[23] F. W. J. Olver, in *Handbook of Mathematical Functions*, edited by M. Abramowitz and I. A. Stegun (Dover, New York, 1964).

[24] I. J. Berson, J. Phys. B **8**, 3078 (1975); another approach to this interaction has been presented by J. Z. Kamiński, Phys. Rev. A **52**, 4976 (1995).

[25] The problem of zero-range potential in a laser field has also been studied both analytically and numerically in F. H. M. Faisal, Comput. Phys. Rep. **9**, 57 (1989); F. H. M. Faisal, P. Filipowicz, and K. Rzążewski, Phys. Rev. A **41**, 6176 (1990); P. Filipowicz, F. H. M. Faisal, and K. Rzążewski, *ibid.* **44**, 2210 (1991).

[26] A zero-range interaction in an arbitrary $\boldsymbol{d}$-dimensional space has been discussed by K. Wódkiewicz, Phys. Rev. A **43**, 68 (1990); and by K. Krajewska, Master's thesis, Warsaw University, Warszawa, 1999 (unpublished).